Supporting Information for

Development of pan-anti-SARS-CoV-2 agents through allosteric inhibition of nsp14/nsp10 complex

Jingxin Chen[1], Ying Zhou[1], Xueying Wei[1,2], Xiaohan Xu[1], Zhenzhi Qin[2], Chon Phin Ong[3], Zi-Wei Ye[3], Dong-Yan Jin[3], Bernard Boitrel[4], Shuofeng Yuan[2], Jasper F.-W. Chan[2], Hongyan Li[1,*], and Hongzhe Sun[1,*]

1, Department of Chemistry, State Key Laboratory of Synthetic Chemistry and CAS-HKU Joint Laboratory of Metallomics on Health and Environment, The University of Hong Kong, Pokfulam Road, Hong Kong 999077, P. R. China

2, Department of Microbiology, The University of Hong Kong, Sassoon Road, Hong Kong 999077, P. R. China

3, School of Biomedical Sciences, The University of Hong Kong, Sassoon Road, Hong Kong 999077, P. R. China

4, University of Rennes, CNRS, ISCR (Institut des Sciences Chimiques de Rennes)-UMR 6226, 35000 Rennes, France

* Correspondence: Hongzhe Sun (hsun@hku.hk); Hongyan Li (hylichem@hku.hk)

TABLE OF CONTENT

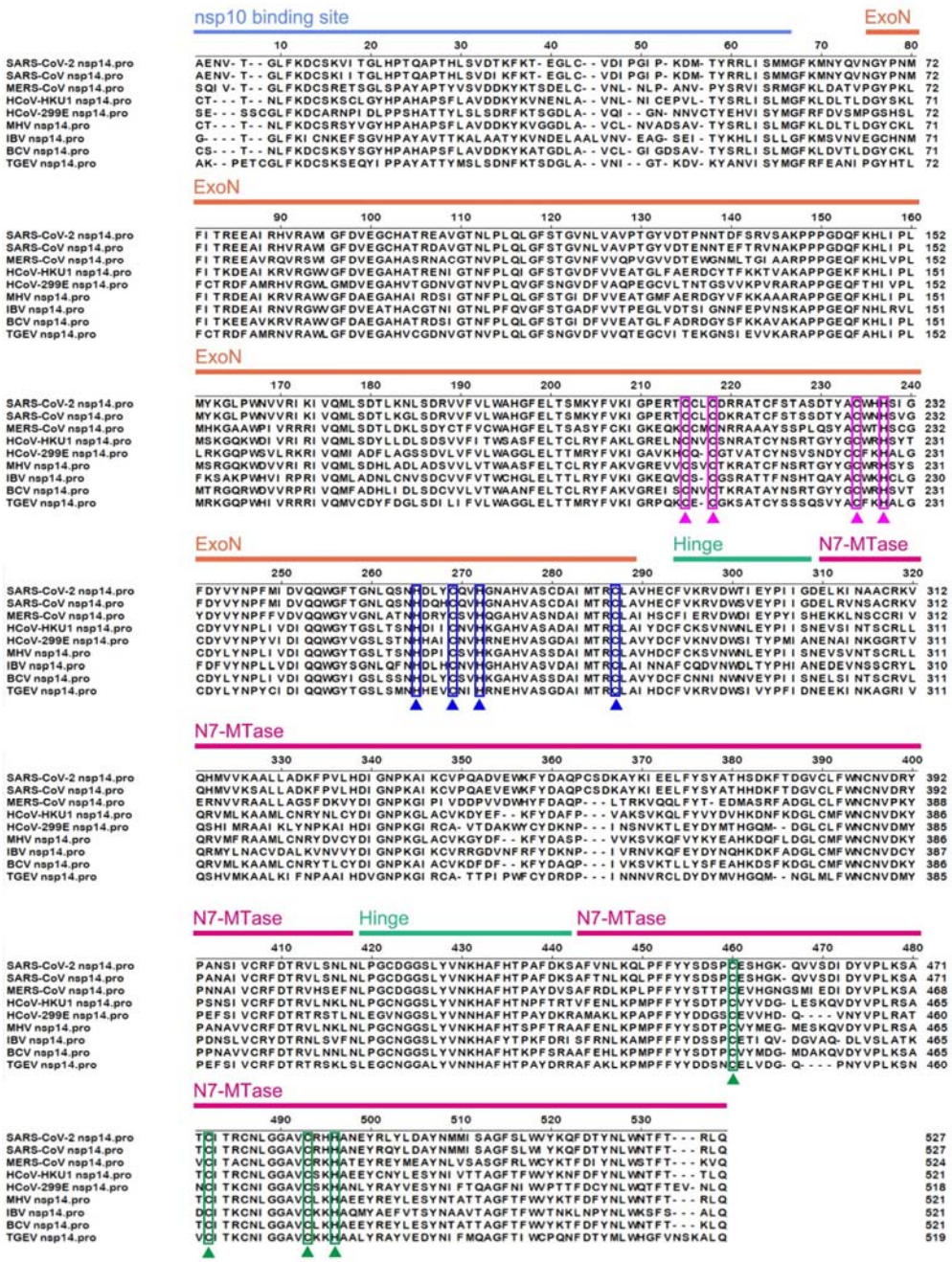

Figure S1. Sequence alignment of nsp14 from selected coronaviruses using MegAlign (DNASTAR) software. Sequences of the ExoN and N7-MTase domains in MERS-CoV (NC-019843), SARS-CoV-2 (NC_045512.2), SARS-CoV (NC_004718.3), HCoV-HKU1 (NC_006577.2), MHV (NP_045299.2), HCoV-229E (NC_002645.1), IBV (NC_001451.1), BCV (NP_150073.3), TGEV (AJ271965.2), and were used for the analysis. Residues involved in the formation of three zinc fingers are marked with pink, blue and green triangles.

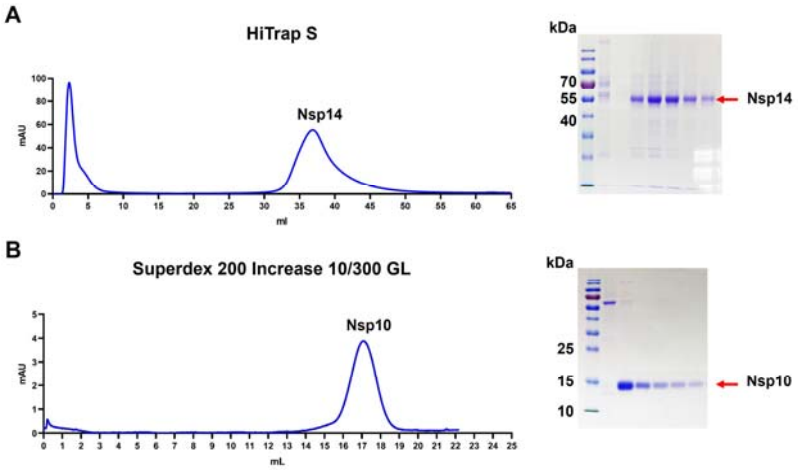

Figure S2. Expression and purification of SARS-CoV-2 nsp10 and nsp14. (A) Nsp14 was purified by HiTrap S ion-exchange column. (B) nsp10 was purified by Superdex 200 Increase 10/300 GL column. Each band on SDS-PAGE represents samples collected from FPLC at different time points of the protein elution peaks.

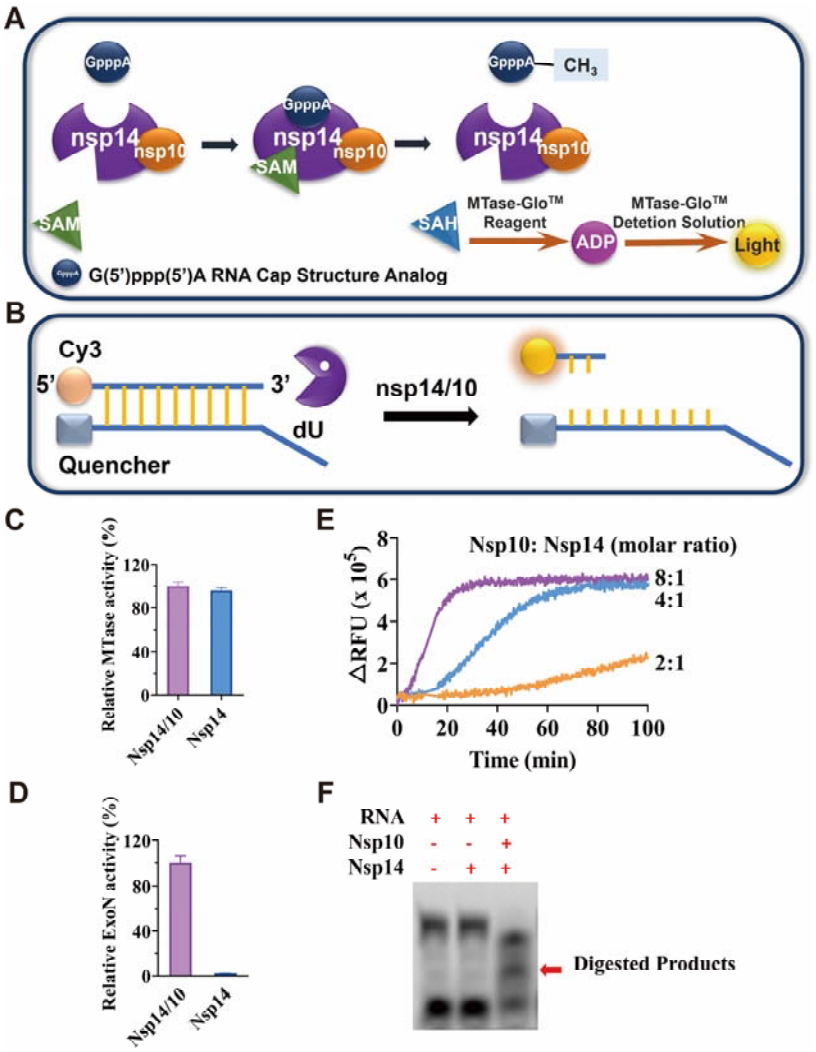

Figure S3. MTase-Glo™ methyltransferase assay and FRET-based exoribonuclease assay for purified nsp14. (A) Outline of bioluminescence assay for nsp14 methyltransferase activity. (B) Outline of FRET-based assay for nsp14 exoribonuclease activity. (C) Relative MTase activity of nsp14 in the absence and presence of nsp10 (n = 3). (D) Fluorescent signal produced by the nucleolytic cleavage of nsp14/nsp10 complex in ExoN assay at different molar ratios of nsp14: nsp10 (n = 3). (E-F) Relative ExoN activity of nsp14 in the absence and presence of nsp10. ExoN assay samples were subjected to 20% Urea-PAGE.

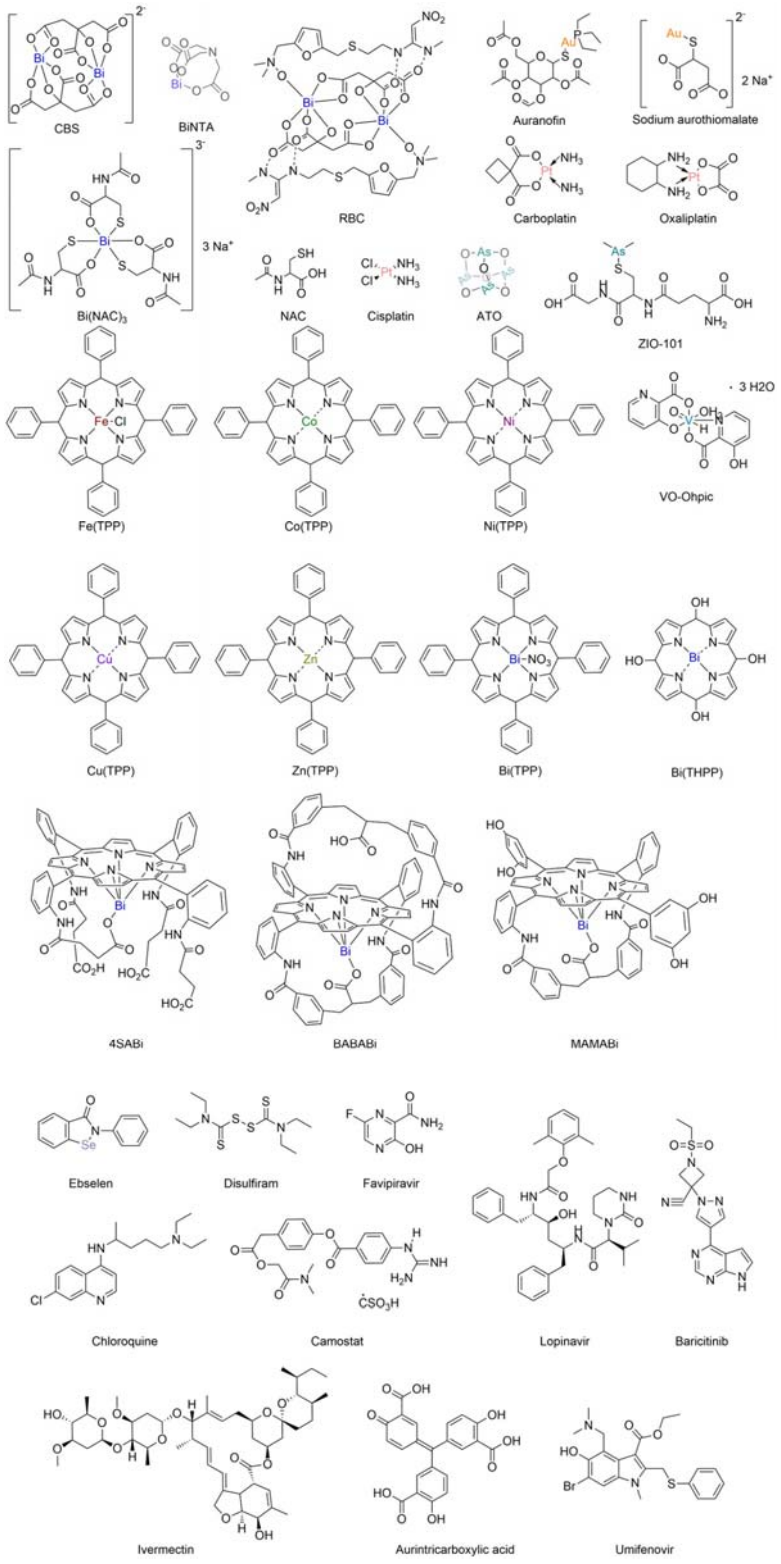

Figure S4. Chemical structures of selected metal-based compounds and potential organic antiviral compounds[1-10].

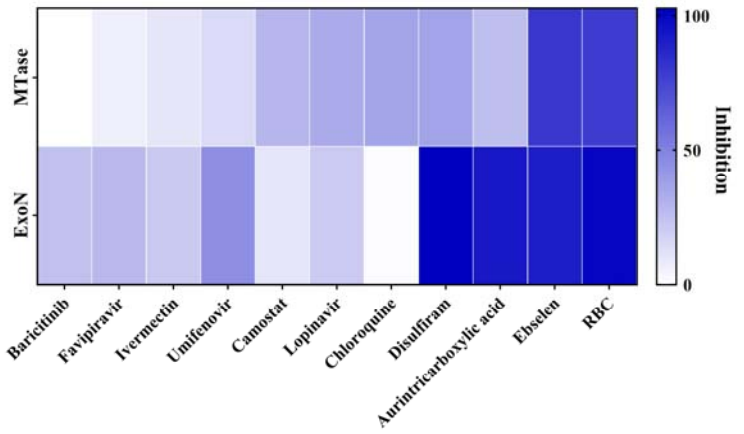

Figure S5. SARS-CoV-2 nsp14/nsp10 as a potential target of organic compounds against SARS-CoV-2 compared with RBC. Relative percentages of inhibition on methyltransferase and exoribonuclease activity of nsp14 (1 μM and 200 nM, respectively) by small organic molecular compounds (n = 3). Compounds were used at a 50:1 molar ratio of compound: nsp14.

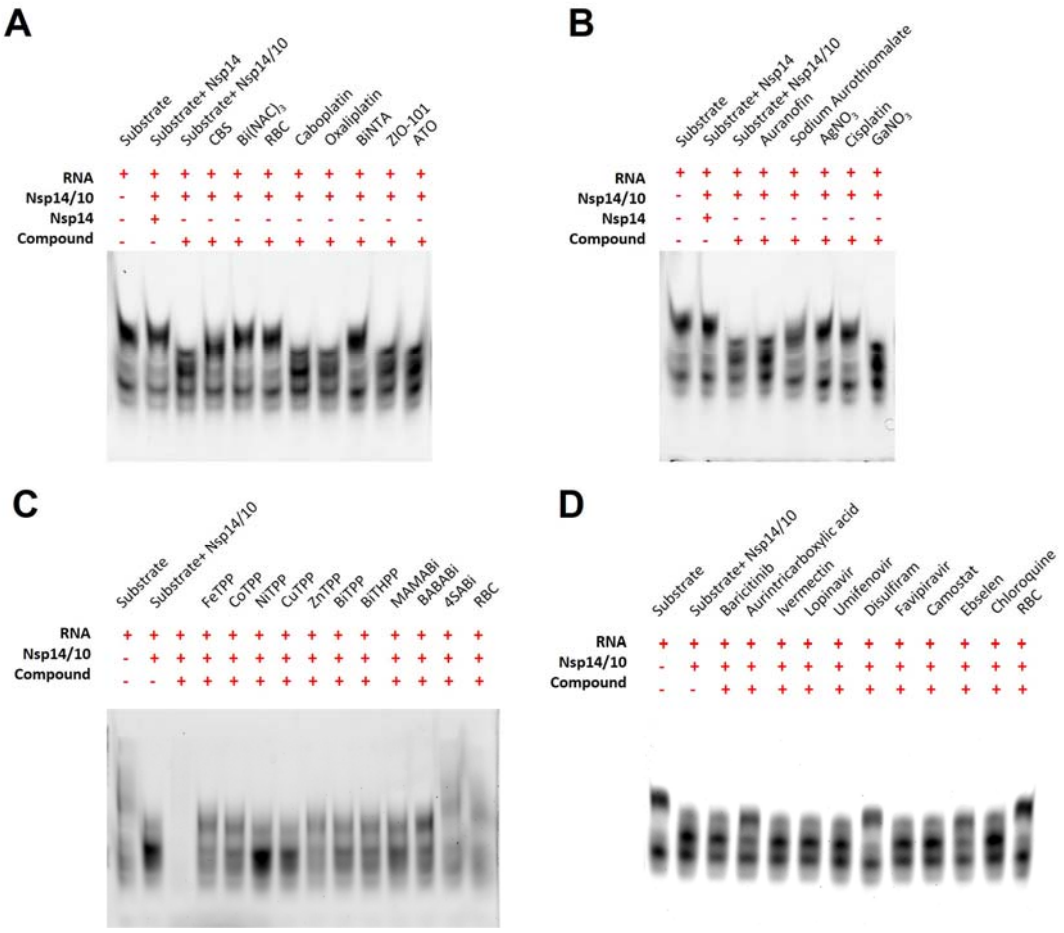

Figure S6. Primary screening of potential inhibitors of nsp14/nsp10 exoribonuclease. FRET-based ExoN assay samples in primary screening were subjected to 20% Urea-PAGE.

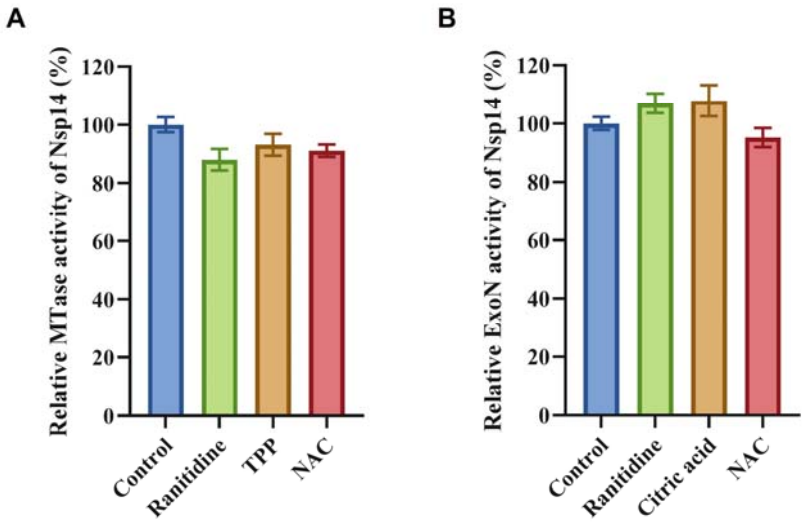

Figure S7. Influence of different ligands on nsp14 activity. MTase (A) and ExoN (B) activity of SARS-CoV-2 nsp14 in the presence of 50 molar equivalents of ligands of bismuth-based compounds (n = 3).

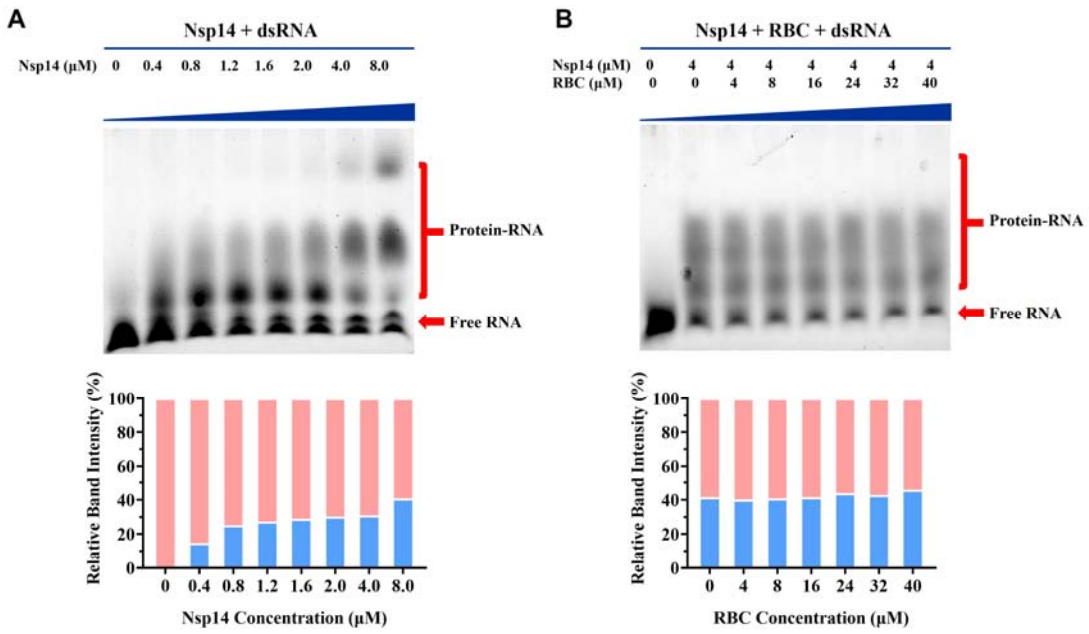

Figure S8. Influence of RBC on the binding of SARS-CoV-2 nsp14 to ExoN substrates. (A) Binding of ExoN dsRNA substrates to SARS-CoV-2 nsp14 at varying concentrations as indicated. (B) Binding of ExoN dsRNA substrates to nsp14 in the presence of RBC at varying concentrations as indicated. Relative band intensities were quantified by ImageJ.

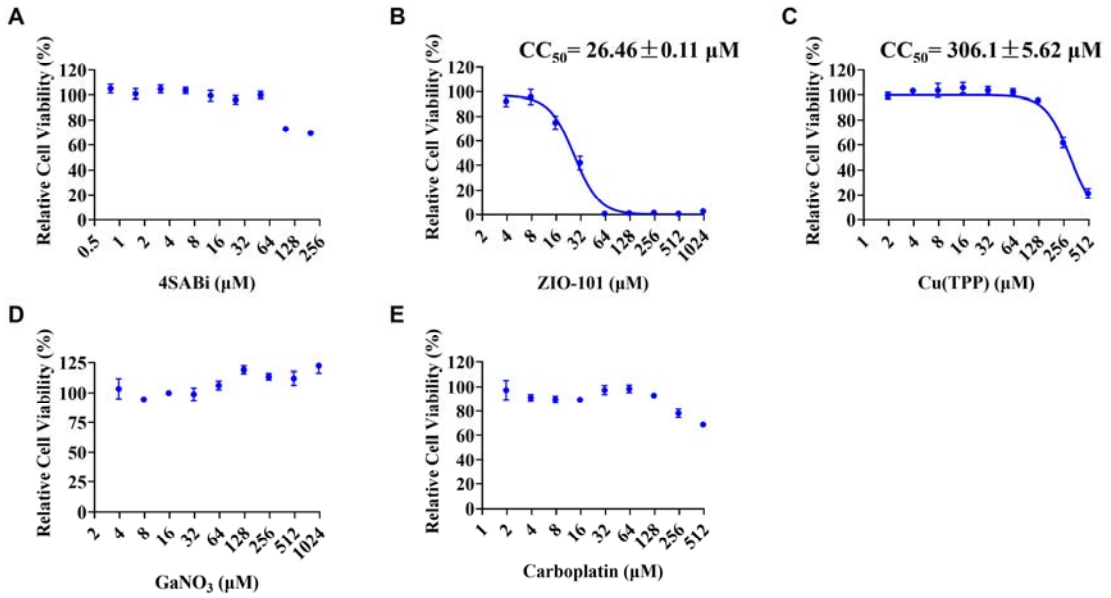

Figure S9. Cytotoxicity of SARS-CoV-2 nsp14 inhibitors against Vero E6 cells (n = 3). CC_{50} values are presented as mean values ± SD.

Table S1. Substrate oligonucleotides.

Oligo	Substrate	Oligo sequence (5'→3')
i	Top Cy3 RNA	Cy3-GGUAGUAAUCCGCUC
ii	Bottom quencher RNA	UUUUUUUUUUUUUUUUUUUUGAGCGGAUUACUACUACC-BHQ-2

Table S2. IC_{50} of the selected compounds against MTase and ExoN activities of nsp14/nsp10.

Compounds	IC_{50} of MTase activity (μM)	IC_{50} of ExoN activity (μM)
RBC	1.03±0.24	0.53±0.07
$Bi(NAC)_3$	1.33±0.26	0.80±0.06
4SABi	1.36±0.28	0.84±0.04
CBS	2.04±0.05	2.08±0.60
BABABi	5.48±0.76	3.76±0.55
Bi(THPP)	3.47±0.85	N.D*
Bi(NTA)	N.D	5.11±2.29
$AgNO_3$	1.57±0.14	0.95±0.04
Cisplatin	5.48±0.26	2.00±0.14
Zn(TPP)	N.D	6.02±0.38
Fe(TPP)	N.D	10.84±0.71

* N.D: not determined.

Table S3. K_m and V_{max} values of nsp14 MTase activity upon Bi(III) treatment.

	SAM-dependent			G(5')ppp(5')A RNA analog-dependent			
4SABi: Nsp14 (Molar ratio)	0	3	6	0	1	3	6
V_{max} (nM/min)	338.8±2.8	282.8±7.1	215.0±5.4	424.3±5.8	336.4±11.9	287.6±3.5	265.7±2.6
K_m (μM)	1.4±0.2	1.3±0.1	1.2±0.1	1.3±0.1	1.4±0.1	1.0±0.1	1.0±0.1

Table S4. K_m and V_{max} values of nsp14/nsp10 ExoN activity upon Bi(III) treatment.

RBC: Nsp14 (Molar ratio)	0	5	10
V_{max} (nM/min)	58.8±4.2	48.3±1.8	33.4±0.4
K_m (μM)	259.9±3.1	267.7±6.9	261.5±6.2

SI REFERENCES

(1) Udwadia, Z. F.; Singh, P.; Barkate, H.; Patil, S.; Rangwala, S.; Pendse, A.; Kadam, J.; Wu, W.; Caracta, C. F.; Tandon, M. Efficacy and safety of favipiravir, an oral RNA-dependent RNA polymerase inhibitor, in mild-to-moderate COVID-19: A randomized, comparative, open-label, multicenter, phase 3 clinical trial. *Int. J. Infect. Dis.* **2021**, *103*, 62-71.

(2) Refat, M. S.; Sedayo, A. A.; Sayqal, A.; Alharbi, A.; Katouah, H. A.; Abumelha, H. M.; Alzahrani, S.; Alkhatib, F.; Althagafi, I.; El-Metwaly, N. Aurintricarboxylic acid and its metal ion complexes in comparative virtual screening versus Lopinavir and Hydroxychloroquine in fighting COVID-19 pandemic: Synthesis and characterization. *Inorg. Chem. Commun.* **2021**, *126*, 108472.

(3) Muralidharan, N.; Sakthivel, R.; Velmurugan, D.; Gromiha, M. M. Computational studies of drug repurposing and synergism of lopinavir, oseltamivir and ritonavir binding with SARS-CoV-2 protease against COVID-19. *J. Biomol. Struct. Dyn.* **2021**, *39* (7), 2673-2678.

(4) López-Medina, E.; López, P.; Hurtado, I. C.; Dávalos, D. M.; Ramirez, O.; Martínez, E.; Díazgranados, J. A.; Oñate, J. M.; Chavarriaga, H.; Herrera, S.; Parra, B.; Libreros, G.; Jaramillo, R.; Avendaño, A. C.; Toro, D. F.; Torres, M.; Lesmes, M. C.; Rios, C. A.; Caicedo, I. Effect of ivermectin on time to resolution of symptoms among adults with mild COVID-19. *JAMA* **2021**, *325* (14), 1426.

(5) Kalil, A. C.; Stebbing, J. Baricitinib: the first immunomodulatory treatment to reduce COVID-19 mortality in a placebo-controlled trial. *Lancet Respir. Med.* **2021**, *9* (12), 1349-1351.

(6) Huang, D.; Yu, H.; Wang, T.; Yang, H.; Yao, R.; Liang, Z. Efficacy and safety of umifenovir for coronavirus disease 2019 (COVID-19): A systematic review and meta-analysis. *J. Med. Virol.* **2021**, *93* (1), 481-490.

(7) Hoffmann, M.; Hofmann-Winkler, H.; Smith, J. C.; Krüger, N.; Arora, P.; Sørensen, L. K.; Søgaard, O. S.; Hasselstrøm, J. B.; Winkler, M.; Hempel, T.; Raich, L.; Olsson, S.; Danov, O.; Jonigk, D.; Yamazoe, T.; Yamatsuta, K.; Mizuno, H.; Ludwig, S.; Noé, F.; Kjolby, M.; Braun, A.; Sheltzer, J. M.; Pöhlmann, S. Camostat mesylate inhibits SARS-CoV-2 activation by TMPRSS2-related proteases and its metabolite GBPA exerts antiviral activity. *EBioMedicine* **2021**, *65*, 103255.

(8) Chen, T.; Fei, C.-Y.; Chen, Y.-P.; Sargsyan, K.; Chang, C.-P.; Yuan, H. S.; Lim, C. Synergistic Inhibition of SARS-CoV-2 Replication Using Disulfiram/Ebselen and Remdesivir. *ACS Pharmacol. Transl. Sci.* **2021**, *4* (2), 898-907.

(9) Axfors, C.; Schmitt, A. M.; Janiaud, P.; Van'T Hooft, J.; Abd-Elsalam, S.; Abdo, E. F.; Abella, B. S.; Akram, J.; Amaravadi, R. K.; Angus, D. C.; Arabi, Y. M.; Azhar, S.; Baden, L. R.; Baker, A. W.; Belkhir, L.; Benfield, T.; Berrevoets, M. A. H.; Chen, C.-P.; Chen, T.-C.; Cheng, S.-H.; Cheng, C.-Y.; Chung, W.-S.; Cohen, Y. Z.; Cowan, L. N.; Dalgard, O.; De Almeida E Val, F. F.; De Lacerda, M. V. G.; De Melo, G. C.; Derde, L.; Dubee, V.; Elfakir, A.; Gordon, A. C.; Hernandez-Cardenas, C. M.; Hills, T.; Hoepelman, A. I. M.; Huang, Y.-W.; Igau, B.; Jin, R.; Jurado-Camacho, F.; Khan, K. S.; Kremsner, P. G.; Kreuels, B.; Kuo, C.-Y.; Le, T.; Lin, Y.-C.; Lin, W.-P.; Lin, T.-H.; Lyngbakken, M. N.; McArthur, C.; McVerry, B. J.; Meza-Meneses, P.; Monteiro, W. M.; Morpeth, S. C.; Mourad, A.; Mulligan, M. J.; Murthy, S.; Naggie, S.; Narayanasamy, S.; Nichol, A.; Novack, L. A.; O'Brien, S. M.; Okeke, N. L.; Perez, L.; Perez-Padilla, R.; Perrin, L.; Remigio-Luna, A.; Rivera-Martinez, N. E.; Rockhold, F. W.; Rodriguez-Llamazares, S.; Rolfe, R.; Rosa, R.; Røsjø, H.; Sampaio, V. S.; Seto, T. B.; Shahzad, M.; Soliman, S.; Stout, J. E.; Thirion-Romero, I.; Troxel, A. B.; Tseng, T.-Y.; Turner, N. A.; Ulrich, R. J.; Walsh, S. R.; Webb, S. A.; Weehuizen, J. M.; Velinova, M.; Wong, H.-L.; Wrenn, R.; Zampieri, F. G.; Zhong, W.; Moher, D.; Goodman, S. N.; Ioannidis, J. P. A.; Hemkens, L. G. Mortality outcomes with hydroxychloroquine and chloroquine in COVID-19 from an international collaborative meta-analysis of randomized trials. *Nat. Commun.* **2021**, *12* (1), 2349.

(10) Amporndanai, K.; Meng, X.; Shang, W.; Jin, Z.; Rogers, M.; Zhao, Y.; Rao, Z.; Liu, Z.-J.; Yang, H.; Zhang, L.; O'Neill, P. M.; Samar Hasnain, S. Inhibition mechanism of SARS-CoV-2 main protease by ebselen and its derivatives. *Nat. Commun.* **2021**, *12* (1), 3061.